Research Square

Preprints are preliminary reports that have not undergone peer review.
They should not be considered conclusive, used to inform clinical practice,
or referenced by the media as validated information.

Vertical Graphene Arrays for AC Line-Filtering Capacitors

Jin Zhang (jinzhang@pku.edu.cn)
Peking University https://orcid.org/0000-0003-3731-8859
Shichen Xu
Peking University
Yeye Wen
Peking University
Zhuo Chen
Peking University
Nannan Ji
Beijing Graphene Institute (BGI)
Mingmao Wu
Fuzhou University
Zhigang Zou
Nanjing University
Liangti Qu
Tsinghua University https://orcid.org/0000-0002-0161-3816

Article

Keywords: Electrode Area, Ion Transport, Chemical Vapor Deposition, Aluminum Electrolytic Capacitor

Posted Date: July 6th, 2021

DOI: https://doi.org/10.21203/rs.3.rs-632738/v1

License: This work is licensed under a Creative Commons Attribution 4.0 International License.
Read Full License

Vertical Graphene Arrays for AC Line-Filtering Capacitors

Shichen Xu[1,3], Yeye Wen[1,3], Zhuo Chen[1,3], Nannan Ji[3], Zhigang Zou[2], Mingmao Wu[2], Liangti Qu[5]*, Jin Zhang[1,3,4]**

S. C. Xu, Dr. Y. Y. Wen, Dr. Z. Chen, Prof. J. Zhang
[1] Center for Nanochemistry
Beijing Science and Engineering Center for Nanocarbons
Beijing National Laboratory for Molecular Sciences
College of Chemistry and Molecular Engineering
Peking University
Beijing 100871, P. R. China
E-mail: jinzhang@pku.edu.cn

Prof. Z. G. Zou, Prof. M. M. Wu
[2]College of Chemistry
Fuzhou University
Fuzhou 350108, P. R. China
E-mail: wumm20@fzu.edu.cn

S. C. Xu, Dr. Y. Y. Wen, Dr. Z. Chen, N. N. Ji, Prof. J. Zhang
[3] Beijing Graphene Institute (BGI), Beijing, 100095, P. R. China

Prof. J. Zhang

[4]School of Materials Science and Engineering

Peking University
Beijing 100871, P. R. China
E-mail: jinzhang@pku.edu.cn

Prof. L. T. Qu,
[5] Department of Chemistry,
State Key Laboratory of Tribology,
Department of Mechanical Engineering
Tsinghua University
Beijing 100084, P. R. China
E-mail: lqu@tsinghua.edu.cn

Abstract

High-frequency responsive electrochemical capacitor (EC), which can convert alternating current (AC) in the circuit to direct current (DC), is an ideal filtering capacitor with lightweight superiority to replace the bulky aluminum electrolytic capacitor (AEC). However, current electrodes are difficult to achieve high energy density and high-frequency response properties simultaneously, primarily due to the electrode structure dilemmas of maximizing the electrode area or accelerating the ion transport. Herein, strictly vertical graphene arrays (SVGAs) directly prepared by electric-field-assisted plasma enhanced chemical vapor deposition have been successfully designed as the main electrode material of ECs to ensure the ions rapidly adsorb/desorb within the richly available surface spaces. The SVGAs exhibit an excellent specific areal capacitance of 1.72 $mF \cdot cm^{-2}$ at $\Phi_{120} = 80.6°$ even after 500,000 cycles in the aqueous ECs, which is far better than that of most quasi-vertical electrodes and carbon-related materials. Impressively, the output voltage could also be improved to 2.5 V when using the organic electrolyte, and an ultra-high energy density of 4.75 $mF \cdot V^2 \cdot cm^{-2}$ at $\Phi_{120} = 80.6°$ can also be handily achieved. Moreover, both aqueous and organic ECs-SVGAs can well smooth arbitrary AC waveforms into DC signals, indicating that ECs-SVGAs have colossal potentials to replace outmoded AECs.

Introduction

With the rapid development of portable electronic products, wearable devices, electric vehicles, and other energy storage devices toward lightweight and

miniaturization, electrochemical capacitors (ECs) with fast rate capability, appreciable capacitance density, long cycling life, and appropriate flexibility have attracted extensive attention[1-5]. In particular, the high-frequency responsive EC, which smooths the leftover alternate currents (AC) ripples into direct currents (DC) in line-powered devices at 120 Hz, is an encouraging alternate for the bulky and rigid aluminum electrolytic capacitor (AEC)[6-9]. However, integration of high energy density and high frequency response properties within a tiny EC device still remains a challenge, which lies in mutually exclusive requirements for complex electrode structures[10-13]. For instance, although common mesoporous electrodes possess an enormous specific surface area (SSA) and high capacitance density, the tortuous structures inevitably make the ion transport sluggish, thus a slower response to the frequency variation[14-16].

Given this, a myriad of electrode materials with elaborate structures have been developed to balance the trade-offs between the ion transport property and capacitance density, including the vertically aligned arrays, large porous films, onion-like nanoparticles, edge-oriented coating, and their composite assemblies[17-28]. Among them, large porous structures are of advantage for rapid ion transport, which enables the phase angle value at 120 Hz (Φ_{120}) to reach −80° (the Φ_{120} close to −90° represents a good capacitive behavior)[14, 15, 25, 26, 29, 30]. However, the zigzag network and overlarge pore size make the porous structures unsuitable for maximizing spatial charge storage. The onion-like, edge-oriented, or other particles with a large external surface and edge area can provide additional ion adsorption/desorption sites, enlarging the capacitance at the high-frequency region[7, 18, 31-33]. Nevertheless, it always requires another scaffold to

support these nanosized particles, leading to a critical influence on the high-frequency response. In contrast, strictly vertical arrays holding straightly open channels and abundant charge storage surfaces are ideal electrodes for excellent AC line filtering. However, traditional vertical electrodes achieved the high-frequency response property with limited electrode thickness (~2 μm)[17, 34-37]. With the thickness increasing, the quasi-vertical electrode surfaces will geometrically restack, causing some of them are partially inaccessible to the electrolyte. Hence, realizing fast frequency response capability while high capacitance density for the AC filtering ECs is still a significant and demanding task.

Herein, we developed an electric-field assisted plasma-enhanced chemical vapor deposition (EF-PECVD) method to grow strictly vertical graphene arrays (SVGAs) as electrode materials of ECs. In the SVGAs, graphene sheets are arranged vertically and bonded to each other, forming a conductive network in the horizontal direction and micro-channel in the vertical direction. And benefiting from electric-field inducing, the vertical morphology of SVGAs could surpass a height of ~30 μm without any bending. Moreover, free-standing graphene sheets and the connection between directly grown graphene and the current collector endow the capacitors with high SSA and excellent conductivity. Hence, SVGAs exhibit an excellent specific areal capacitance (C_A) of 1.72 mF cm^{-2} at Φ_{120} = 80.6° in aqueous ECs, which is over 19 times higher than that of graphene sheets grown with traditional PECVD and better than that of all the quasi-vertical electrodes. Moreover, the output voltage could also be improved to 2.5 V by using the organic electrolyte. Accordingly, an ultra-high energy density of 4.75 mF V^2

cm^{-2} at Φ_{120} = 80.6° can be achieved. Furthermore, both aqueous and organic SVGAs-ECs can well smooth arbitrary AC waveforms into DC signals, demonstrating outstanding filtering functions in diversified scenarios. All of these excellent properties contribute SVGAs as an irreplaceable electrode material for future filter capacitors.

Results and Discussion

Construction of SVGAs and ECs

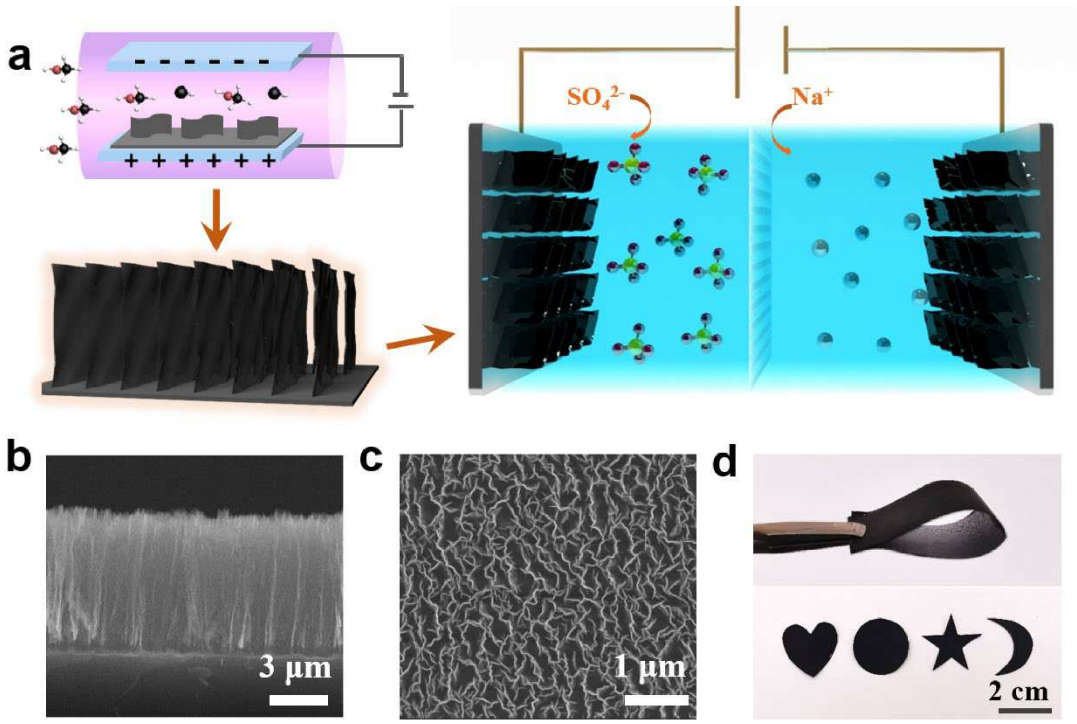

Figure 1. Synthetic procedure and morphology characterization of electrode materials for EC. **a** Schematic illustrations of EF-PECVD procedure for growth of SVGAs and construction of SVGAs based EC. **b, c** sectional-view and top-view SEM images of SVGAs. **d** digital photo of SVGAs electrode with flexibility and machinability.

Current vertical electrodes, including the most common electrochemical deposited

reduced graphene oxide (ErGO) and vertically oriented graphene nanosheets (VOGNs) fabricated by radio frequency plasma enhanced chemical vapor deposition (RF-PECVD), exhibit a quasi-perpendicular arrangement, which makes the electrodes suffer from restacking with increasing electrode thicknesses and leads to the limited accessible electrode surface areas and heavily intensified electrolyte resistance[17, 34-36]. Hence, the graphene arrays with strictly vertical channels are connected, which allows the ions to quickly reach the whole pores regardless of electrode height increasing. The overall synthetic procedure for the growth of SVGAs and preparation of flexible ECs constructed by SVGAs are illustrated in **Figure 1a**. Unlike the ErGO or VOGNs, the SVGAs are prepared by a homemade EF-PECVD setup equipped with two parallel electrode pads (upper-left in Figure 1a) which induce a constant vertical electric field[38]. And during the growth procedure, the reactive carbon species generated from plasma bombardment can continuously converge on the graphene edges along with the vertical electric field orientation, thus forming a strict 90° graphene wall on the substrates (lower-left in Figure 1a). Typical side-view and top-view scanning electronic microscope (SEM) images confirm the vertical structure of SVGAs (**Figure 1b** and **1c**). In side-view SEM image, SVGAs represent a free-standing structure, in which all graphene sheets stand vertically on substrates without any tortuosity. Meanwhile, only edges of the graphene sheets could be observed in top-view SEM, also indicating SVGAs exhibit a good perpendicular morphology. Impressively, the electric field could maintain the excellent vertical structure of SVGAs up to 30 μm or even higher (**Figure S1**), which is of good crystalline quality and has no metal and other impurities (**Figure**

S2). Moreover, the SVGAs exhibit small pore sizes (~500 nm) with abundant active edges and non-agglomerated morphology (**Figure 1c**). These features benefit high-frequency electrochemical processes with large specific capacitance densities. Besides, the growth of SVGAs is a low temperature, catalyst-free, universal, and easily scale-up procedure, making it possible to grow a large area SVGAs electrode on various substrates (e.g., copper foil, nickel foil, and graphite foil) with flexibility and arbitrary shapes (**Figure 1d** and **Figure S3**). Finally, the ECs with sandwich configuration were prepared by face to face placing two identical electrodes, and exhibit a compact and portable appearance (the right column of **Figure 1a** and **Figure S4**), delivering good compatibility with miniaturized electronic circuits.

Comparison between SVGAs and quasi-vertical GAs

To elucidate the structural advantage of SVGAs, the quasi-vertical GAs (QVGAs) with the same height were prepared for comparison. **Figure 2a** and **2b** display the cross-sectional microscope images of two different vertical electrode materials grown by PECVD without and with an additional electric field. The morphology of QVGAs is challenging to be accurately controlled in traditional PECVD. At the initial growth stage, QVGAs exhibit a quasi-vertical structure. As the growth time increases, the graphene sheets will overlap and splice with each other and eventually form a dense three-dimensional nanowall structure, (**Figure 2a**) in sharp contrast to the 90° vertical SVGAs. (**Figure 2b**) Their morphological characteristics are also verified by the low-magnification transmission electron microscopy (TEM) (**Figure S5**). Graphene sheets

in QVGAs are disorderly arranged with a domain size of several hundred nanometers, whereas graphene sheets in SVGAs are aligned in parallel with a lateral dimension of up to several microns.

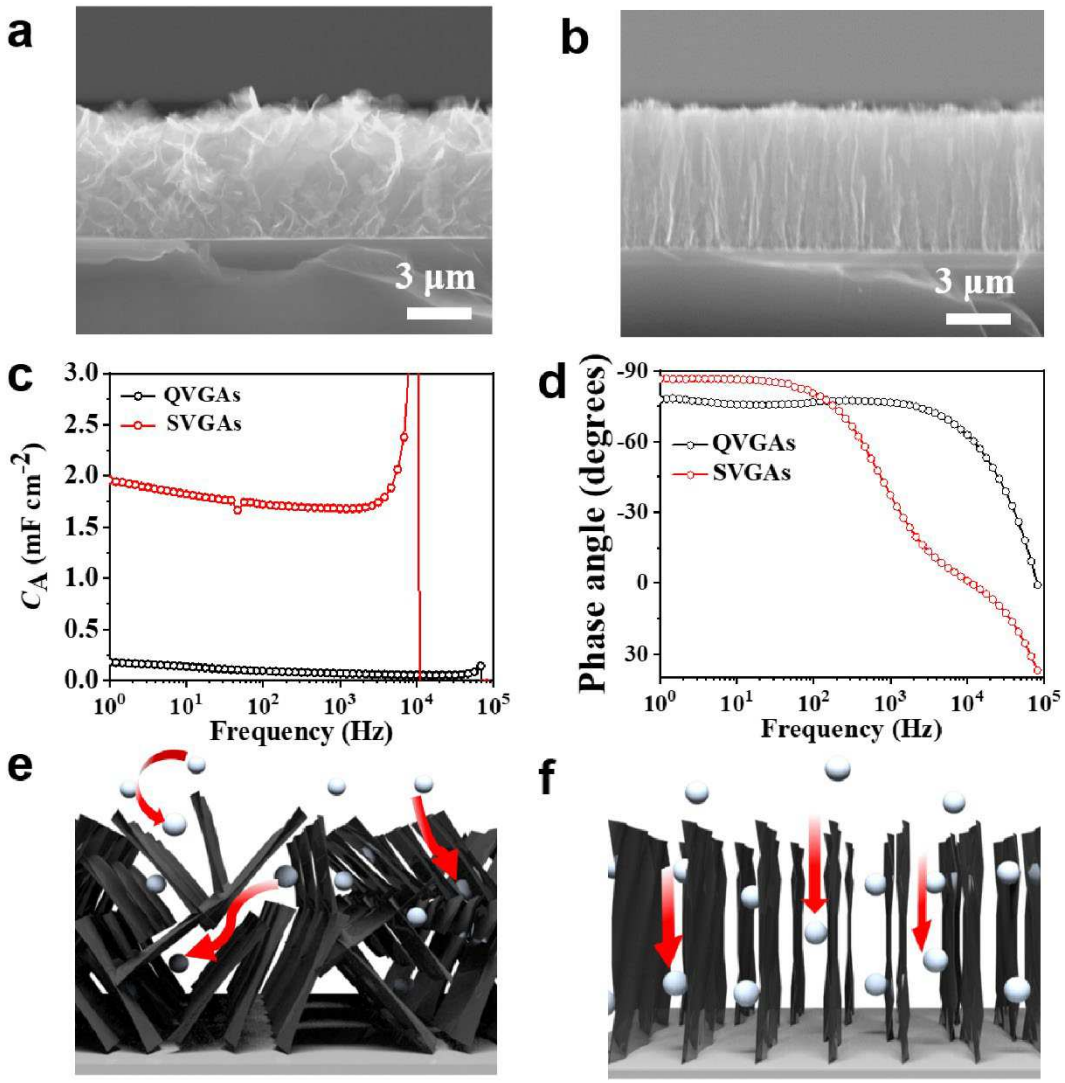

Figure 2. Comparison of structural and electrochemical properties between SVGAs and QVGAs. **a, b** Sectional-view SEM images of QVGAs grown without electrode field and SVGAs grown with electrode field. **c** Plots of phase angle as a function of frequency for EC-SVGAs and EC-QVGAs. **d** Plots of areal specific capacitance (C_A) versus frequency for EC-SVGAs and EC-QVGAs. **e, f** Schematic illustration of ion

diffusion direction based on the morphologies of QVGAs and SVGAs, respectively.

Furthermore, to directly reveal the superiority of SVGAs over QVGAs, the symmetric EC based on SVGAs (EC-SVGAs) and QVGAs (EC-QVGAs) with aqueous electrolytes are fabricated and characterized by the electrochemical impedance spectroscopy (EIS). The electrode thicknesses of both ECs are controlled to be ~6 μm. **Figure 2c** and **2d** display the C_A and phase angle (Φ) as a function of frequency, respectively. Generally, 120 Hz is a critical frequency for evaluating filtering capacitors because the line frequency exactly equals 120 Hz after rectification. At this frequency, SVGAs yields a C_A of 1.72 mF cm^{-2}, which is nearly 19 times higher than that of QVGAs (92 $\mu F \cdot cm^{-2}$). More than that, the Φ_{120} of −80.6° for SVGAs is also closer to −90° compared with that of −77° for QVGAs, demonstrating the outstanding capacitive behavior of SVGAs.

As well known, the structure of electrode materials, which significantly determines the electronic and ionic transport, is closely related to the electrochemical performances. An appropriate electrode material for a high-frequency filtering capacitor should exhibit a large surface area for charge accumulation, high electrical conductivity and smooth ionic transport paths to minimize the resistance, and excellent structural stabilities for long-time service. Accordingly, the better C_A and Φ of EC-SVGAs at 120 Hz should benefit from the unique electrode structure features. As proven by the methylene blue adsorption experiment, the SVGAs exhibit a much larger SSA than that of QVGAs (**Figure S6**), which explains the higher C_A of EC-SVGAs.

Besides, the outstanding capacitive behavior of EC-SVGAs could be ascribed to small equivalent series resistance (ESR) according to phase angle equation (1)

$$\Phi = \arctan\left(\frac{Z''}{Z'}\right) = \arctan\left(\frac{1}{2\pi f R C}\right) \quad (1)$$

where C is the capacitance, f is the frequency, R is the resistance, $Z'' = 1/2\pi fC$ is the imaginary impedance and mainly depends on the frequency variation, $Z' = R$ is the real impedance which is primarily on the ESR in this system. Thus, a smaller Φ (closer to −90°) requires a smaller ESR at a fixed frequency. Meanwhile, the ESR of the ECs could be read out from the Nyquist plots (**Figure S7**), in consistent with the smaller ESR of EC-SVGAs. On this basis, we can conclude the strictly vertical structure and ordered graphene sheets of SVGAs maximize the utilization of surface area and provide the open channels for the shortest straight path of ions, which is in favor of excellent electrochemical performances (**Figure 2f**). In contrast, the agglomerated structure of QVGAs would waste the available charge adsorption surface and restrict the smooth ions transport, further increasing the distance for ion exchange (**Figure 2e**).

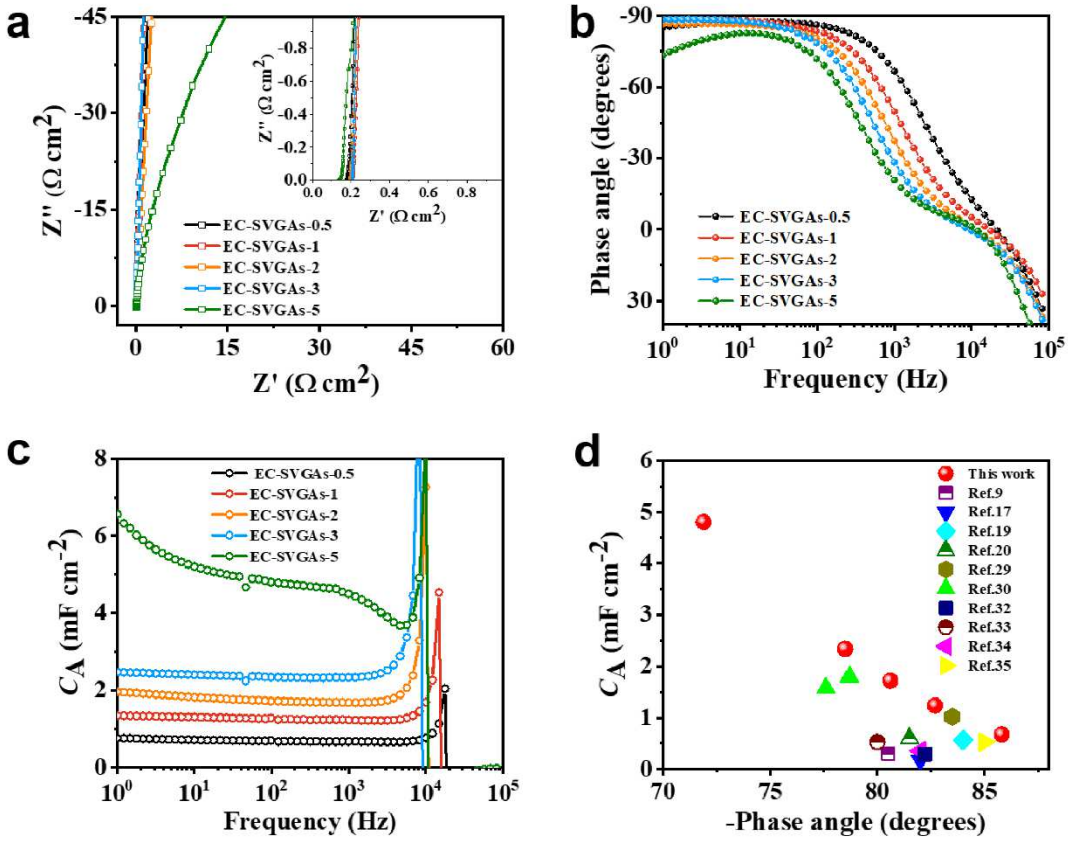

Figure 3. Electrochemical properties of SVGAs based ECs with different height. **a** Nyquist plot of EC-SVGAs with different height; inset: the expanded view at high frequencies. **b** Plots of phase angle as a function of frequency for EC-SVGAs with different height. **c** Plots of areal specific capacitance (CA) versus frequency for EC-SVGAs with different height. **d** Comparison of phase angle and C_A of EC-SVGAs with those of reported carbon related ECs for AC line-filtering.

Electrochemical performances of EC-SVGAs

In addition to the vertical orientation, the height of vertical arrays prepared by EF-PECVD could be easily adjusted by the growth time. As shown in **Figure S8**, when the electric field force is set at 30 V cm^{-1}, the height of the SVGAs increased linearly with

the growth time with an average rate of ~3 μm h^{-1}, from ~1.5 μm in half hour to ~15.0 μm in 5 hours. For clarity, the different SVGAs were nominated as SVGAs-n (n = 0.5, 1, 2, 3, 5), where n represents the growth time. And the EC assembled by the corresponding electrodes with aqueous electrolyte was denoted as EC-SVGAs-n. As shown in Nyquist plots (**Figure 3a**), all the curves exhibit the near-vertical characteristic and miss the semicircle at the high-frequency region, implying the electrochemical process of EC-SVGAs-n is a complete double electric layer mechanism rather than faradic charge transfer reaction. The absence of the 45° line also confirms the channels in the SVGAs-n are straightly open without other micro- or mesoporous structure[39]. Almost the same ohmic resistance of 0.2 Ω cm^2 of EC-SVGAs-n also indicates the contact resistance is unrelated to electrode loading, demonstrating SVGAs always possess straightway vertical construction no matter what height of the electrode. Additionally, the excessive height does influence *Z'* at the low-frequency region, which could also be inferred in the variations of Φ and C_A (**Figure 3b** and **3c**). The lowest Φ_{120} of EC-SVGAs-n is measured as high as −85.8°, which is even better than commercial AECs (22 μF) (**Figure S9**). With the increase of height from 1.5 μm to 15.0 μm, the Φ_{120} slightly decrease in the sequence of −85.8°, −82.7°, −80.6°, −78.5°, and −71.9°, informing increasing resistance caused by additional ion transport distance. Different from Φ, the C_A exhibits an incremental improvement from 0.67 to 4.80 mF·cm^{-2} with the increase of SVGAs height, which should be benefited from the significantly enhanced ion-accessible surface area triggered by SVGAs growth. Although there are some trade-offs between the Φ and C_A, the excellent C_A and Φ of

EC-SVGAs-n still surpass those of the best filtering ECs based on QVGAs and most carbon-related devices reported so far (**Figure 3d** and **Table 1**)[9, 17, 19, 20, 29, 30, 32-35]. In addition, the characteristic frequency (f_o) could be read out from the plots of imaginary capacitances (C'') versus frequency (**Figure S10**). And the relaxation time constant ($\tau_0 = 1/f_o$) of EC-SVGAs-n were calculated to 0.383, 0.826, 0.999, 1.46, and 2.62 μs from n = 0.5 to 5, demonstrating the fast ion adsorption/desorption characteristic.

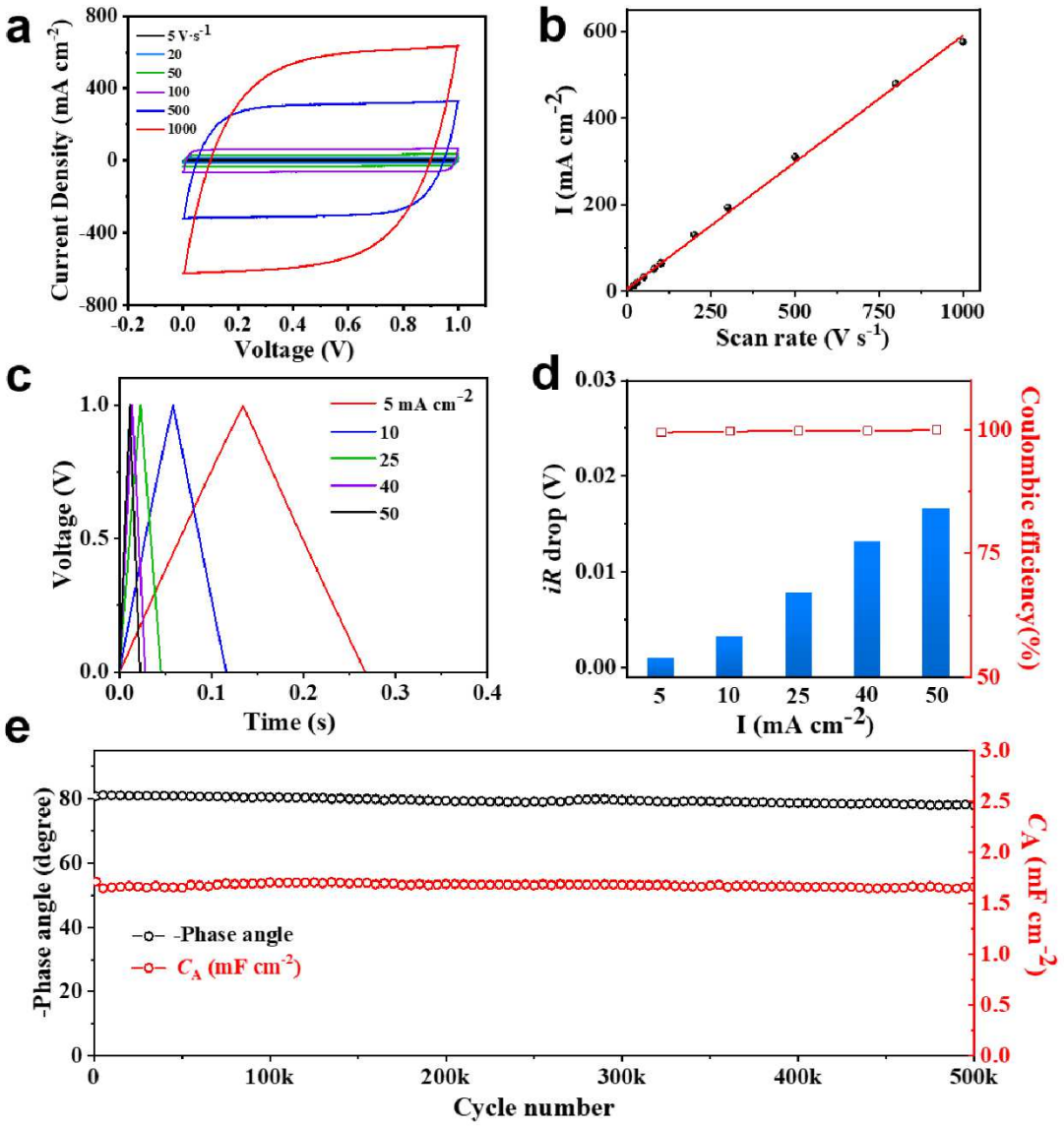

Figure 4. The electrochemical performances of EC-SVGAs-2. **a** CV curves of the EC-SVGAs-2 at scan rate up to 1000 V s^{-1}. **b** Plots of discharge current density at voltage

of 0.5V versus scan rate of the EC-SVGAs-2. **c** Galvanostatic charge–discharge curves at various current densities. **d** Voltage drop and coulombic efficiency versus current densities, respectively. **e** Cycling stability of EC-SVGAs-2.

On this basis of excellent C_A and Φ, the incredible rate capability of EC-SVGAs-n was further characterized by the cyclic voltammetry (CV) tests. Here, the EC-SVGAs-2 was chosen as the main object because it possesses overall best C_A of 1.72 $mF \cdot cm^{-2}$ and Φ of −80.6° at 120 Hz. As shown in **Figure 4a**, the CV profiles of the EC-SVGAs-2 exhibit near rectangular shapes even at an extremely high scan rate of 1000 $V \cdot s^{-1}$. Meanwhile, the discharge current density on the CV curves is linearly proportional to the scan rate in the range of 5 ~ 1,000 $V \cdot s^{-1}$ (**Figure 4b**). These demonstrated the EC-SVGAs-2 could achieve fast electron transport within the electrode materials and maintain good electric double layer capacitive behaviors at ultra-high rate. Besides the CV tests, the galvanostatic charge-discharge (GCD) measurement also confirms the impressive rate capability of EC-SVGAs-2 (**Figure 4c**, **4d and Figure S11**). With the current density up to 50 $mA \cdot cm^{-2}$ corresponding to that the charging and discharging time is less than 22 milliseconds, the EC-SVGAs-2 still shows an ideal isosceles triangular shape with negligible voltage drop (*IR* drop), indicating the 100% coulombic efficiency and ultra-low resistance at rapid charging and discharging process. Otherwise, the intrinsic carbonaceous structure of the SVGAs endows the long-term cycling stability along with nearly unchanged CA and Φ after striking 500 000 cycles (**Figure 4e**).

Considering the possible limitation of aqueous electrolyte (1 V) for high voltage practical application, the higher voltage was eagerly achieved using optional strategies. Organic electrolyte or tandem configuration could stably extend the operation voltage to 2.5 V or X V (X means numbers of series devices) without sacrificing rectangular CV profiles (**Figure S12** and **S13**). Meanwhile, the almost coincident Bode phase diagrams between the high voltage devices and the aqueous EC-SVGAs-2 also indicate their similar capacitive behavior at a wide frequency range (**Figure S14**). Apart from the high-frequency response, the high-capacity characteristic was also retained by utilizing organic electrolyte, which delivers a C_A of 1.52 mF·cm^{-2} comparable to that of EC-SVGAs-2 in aqueous electrolyte (1.72 mF·cm^{-2}) at 120 Hz (**Figure S15**). Combining the 2.5 V working voltage, an ultra-high energy density of 4.75 mF V^2 cm^{-2} at Φ_{120} = 80.6° can be achieved, demonstrating a significant energy storage advantage within a compact space (**Figure S16** and **Table 1**).

Filtering performance of EC-SVGAs

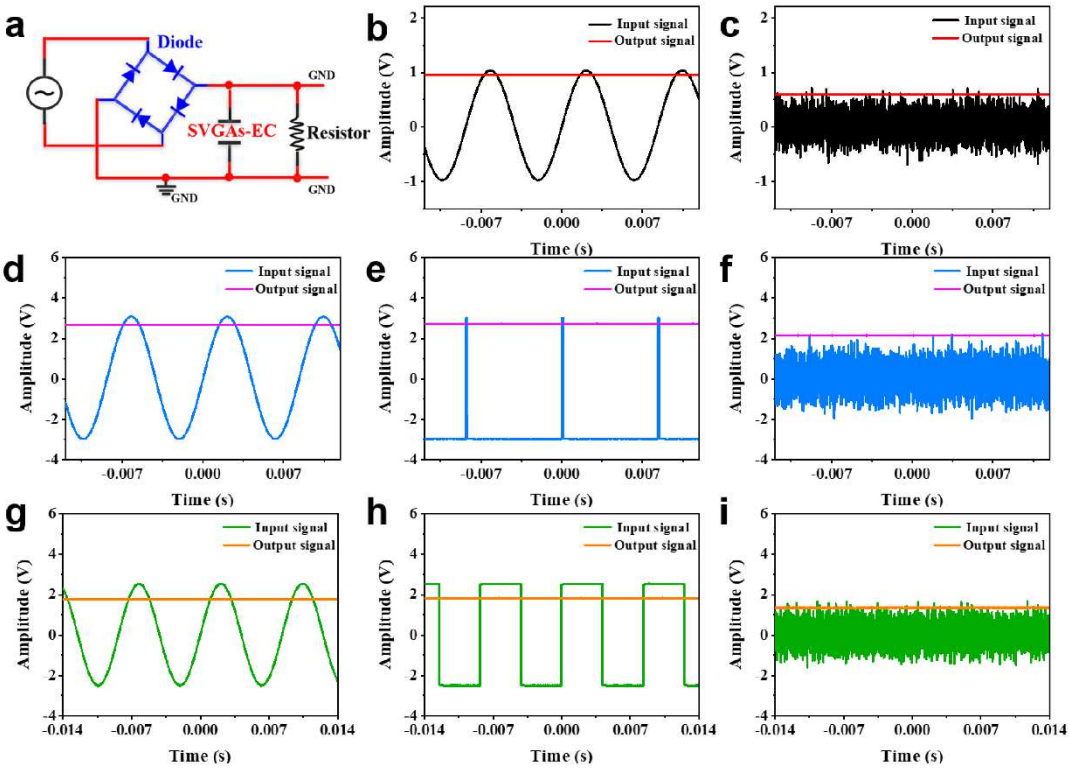

Figure 5. The filtering performances of EC-SVGAs-2. **a** Schematic demonstration of the circuit used for smoothing AC signals. **b, c** Filtering performance of EC-SVGAs unit in aqueous electrolyte. **d-f** Filtering performance of EC-SVGAs connected in series in aqueous electrolyte, **g-i** Filtering performance of EC-SVGAs unit in organic electrolyte.

Given the ultra-high frequency response and large capacity density, which are urgently required for the AC filtering performances with smooth output voltage, the EC-SVGAs was further engineered into the model AC/DC conversion circuit. **Figure 5a** displays the model circuit composed of a full-bridge rectifier, a filtering capacitor (EC-SVGAs), and a loaded resistor (R_L) connected in parallel. As a proof of concept, a series of EC-SVGAs devices with aqueous electrolyte (1 V/0.22 mF), organic

electrolyte (2.5 V/0.19 mF), and tandem configuration was incorporated with 1 MΩ R_L to verify the AC filtering performances. **Figure 5b, 5c**, and **Figure S17** present whether in the aqueous electrolyte or organic electrolyte, the EC-SVGAs can flat the randomly complex AC (60 Hz) to steady DC with inconsiderable ripple voltage, including the sinusoidal square, triangular, and pulse waves. More importantly, even for noise signals with sharply chaotic oscillations, the EC-SVGAs can complete the ripple filtering mission (**Figure 5d**), suggesting the EC-SVGAs have a great potential being applied in pulse environmental energy harvesting equipment requiring specific devices with significant filtering function.

Conclusion

This study accurately controlled the growth orientation of graphene arrays recurring to the electric-field regulated PECVD process and prepared the strictly 90° vertical graphene arrays. Compared with the previous QVGAs, the completely vertical configuration of SVGAs not only ensures straightforward pore structure from the up to down to 30 μm height, but also tremendously enhanced SSA of the materials, thus lead to efficient ion transport and electron transport pathways, and sizeable ion-accessible surface area for the high-frequency charge storage. Accordingly, the EC-SVGAs with aqueous or organic electrolyte is capable of exhibiting excellent C_A, Φ, and energy density at 120 Hz with arbitrary AC filtering performances, which is far better than most ECs based on QVGAs and carbon-related devices, demonstrating the colossal promising of EC-SVGAs for replacement of conventional AECs of practical

importance. Additionally, the electric-field regulations are hopefully extended to other carbonaceous materials and even non-carbon-based materials growth, creating various new functional structures with abundant application potential beyond filtering capacitors.

Experimental Section

Preparation of graphene arrays. A built-in electric field was introduced into conventional inductively coupled PECVD with a frequency of 13.56 MHz, which was purchased from BEST EQUIPMENT (BEQ) in Anhui Province. (**Figure S18**) The electric field was provided by two electrodes connected to a direct current power supply. Voltage can be adjusted easily. In brief, a 2 × 2 cm^2 graphite paper and other substrates were placed in the heating zone of a tube-type PECVD system. The growth temperature is set at ≈650 ºC. After introducing methanol into the system, plasma was then generated with a radio frequency source power of 250 W. When an electric field was introduced into system, oriented VG arrays can be obtained.

Methylene blue adsorption. MB adsorption is a standard method for measuring the specific surface area of graphitic materials, with 1mg of adsorbed MB molecules covering 2.54 m^2 of surface area. The SSA of the vertical graphene was calculated by using the following equation: SSA ($m^2 \cdot g^{-1}$) = 2.54 $\times 10^3$ $\Delta M_{MB}/S_{VG}$, whereΔM_{MB} (g) is the mass change of MB caused by adsorption and S_{VG} (g) is the area of the vertical graphene[40, 41]. The surface areas were calculated by adding a piece of SVGAs or QVGAs into a standard concentration of MB in DI water for a total of 24 h to reach

adsorption equilibrium. The MB concentration was determined through UV – vis spectroscopy of supernatant at a wavelength of 665 nm and compared with the initial standard concentration of MB before interacting with SVGAs or QVGAs.

Fabrication of ECs. An EC-SVGAs-n was assembled by two same SVGAs-n on the graphite foils in the sandwich configuration. Taking the SVGAs-2 as the example, the SVGAs-2 on the graphite foils were cut into pieces with the specific area of 0.5 × 0.5 cm^2. Two pieces of SVGAs-2 were face to face assembled with a porous anodic aluminum oxide 356 membranes (Whatman) separator. The separator was infiltrated by the electrolyte beforehand. 1M Na_2SO_4 and 1M acetonitrile solution of tetraethylammonium-tetrafluoroborate were adopt as the aqueous and organic electrolyte, respectively. The other EC-SVGAs-n and EC-QVGAs were prepared by the same procedures except for the different electrode materials.

Electrochemical Characterizations. The electrochemical characterizations were performed on a CHI 660E workstation (CH Instruments Inc., China). For CV and GCD studies, the window voltages were set from 0 to 3 V. EIS tests were conduct at 5 mV amplitude in the frequency range of 1 ~ 100 000 Hz. The AC-line filtering performances were tested by a 33511B arbitrary function generator (Agilent Technologies Inc., Tektronix, USA), and a GBPC3005W ready-made single-phase silicon bridge rectifier (Sep Electron. Corp., Taibei, China). All the outputs were recorded on a RTB2002 mixed domain oscilloscope (Rohde & Schwarz, Germany).

The specific areal capacitance (C, μF cm^{-2}) of symmetric cell was calculated by:

$$C = -\frac{1}{2\pi f Z''} \quad (2)$$

The specific areal capacitance (C_A, μF cm^{-2}) of electrode was calculated by:

$$C_A = \frac{2C}{S} \quad (3)$$

The real specific areal capacitance (C') was calculated by:

$$C' = -\frac{Z''}{2\pi f |Z|^2 S} \quad (4)$$

The imaginary specific areal capacitance (C'') was calculated by:

$$C'' = \frac{Z'}{2\pi f |Z|^2 S} \quad (5)$$

The τ_0 was derived from the f_o at maximum C'':

$$\tau_0 = \frac{1}{f_0} \quad (6)$$

The areal energy density (E_A) of was calculated by:

$$E_A = \frac{C_A U^2}{2} \quad (7)$$

In the equation above, f is frequency; Z' or Z'' is the real or imaginary impedance; Z is the total impedance; S is the area of electrode; f_o is frequency at maximum C''.

Characterizations. The morphology and detailed structure of VG was investigated by SEM (FEI Quattro S, acceleration voltage 5-10 kV, TEM (FEI Tecnai F20; acceleration voltage 200 kV); Raman spectroscopy (Horiba, LabRAM HR 800, 532 nm laser wavelength), XPS (Kratos Analytical Axis-Ultra spectrometer with Al Kα X-ray source).

Acknowledgements

(The authors thank Yangyong Sun from Peking University, Wei Qiao, and Chao Shen from Beijing Graphene Institute for their kind suggestion and discussion on practical experiment. This work was financially supported by the Ministry of Science and Technology of China (2016YFA0200100 and 2018YFA0703502), the National Natural Science Foundation of China (Grant Nos. 52021006, 51720105003, 21790052, 21974004), the Strategic Priority Research Program of CAS (XDB36030100), and the Beijing National Laboratory for Molecular Sciences (BNLMS-CXTD-202001). This work was also supported by the Open Fund of the Key Lab of Organic Optoelectronics & Molecular Engineering.

Reference

1. Dubal D. P., et al. Towards flexible solid-state supercapacitors for smart and wearable electronics. *Chem. Soc. Rev.* **47**, 2065-2129 (2018).

2. Maher F. E., et al. Laser scribing of high-performance and flexible graphene-based electrochemical capacitors. *Science* **335**, 1326-1330 (2012).

3. Yang X. W., et al. Liquid-Mediated Dense Integration of Graphene Materials for Compact Capacitive Energy Storage. *Science* **341**, 534-537 (2013).

4. Kyerematen N. A., Brousse T. & Pech D. Microsupercapacitors as miniaturized energy-storage components for on-chip electronics. *Nat. Nanotech.* **12**, 7-15 (2017).

5. El-Kady M. F. & Kaner R. B. Scalable fabrication of high-power graphene micro-supercapacitors for flexible and on-chip energy storage. *Nat. Commun.* **4**, 1475 (2013).

6. Wu M. M., et al. Arbitrary waveform AC line filtering applicable to hundreds of volts based on aqueous electrochemical capacitors. *Nat. Commun.* **10**, 2855 (2019).

7. Gund G. S., et al. MXene/Polymer Hybrid Materials for Flexible AC-Filtering Electrochemical Capacitors. *Joule* **3**, 164-176 (2019).

8. Kurra N., Hota M. K. & Alshareef H. N. Conducting polymer micro-supercapacitors for flexible energy storage and Ac line-filtering. *Nano Energy* **13**, 500-508 (2015).

9. Chi F., et al. Graphene-Based Organic Electrochemical Capacitors for AC Line Filtering. *Adv. Energy. Mater.* **7**, 1700591 (2017).

10. Stoller M. D. & Ruoff R. S. Best practice methods for determining an electrode material's performance for ultracapacitors. *Energy Environ. Sci.* **3**, 1294-1301 (2010).

11. Zhang M., et al. An ultrahigh-rate electrochemical capacitor based on solution-processed highly conductive PEDOT:PSS films for AC line-filtering. *Energy Environ. Sci.* **9**, 2005-2010 (2016).

12. Wu Z. S., et al. Graphene-based in-plane micro-supercapacitors with high power and energy densities. *Nat. Commun.* **4**, 2487 (2013).

13. Laszczyk K. U., et al. Lithographically Integrated Microsupercapacitors for Compact, High Performance, and Designable Energy Circuits. *Adv. Energy. Mater.* **5**, 1500741 (2015).

14. Yoo Y., et al. Fast-response supercapacitors with graphitic ordered mesoporous carbons and carbon nanotubes for AC line filtering. *J. Mater. Chem. A* **4**, 5062-5068 (2016).

15. Zhang Z., et al. Scalable fabrication of ultrathin free-standing graphene nanomesh films for flexible ultrafast electrochemical capacitors with AC line-filtering performance. *Nano Energy* **50**, 182-191 (2018).

16. Vlad A. & Balducci A. Supercapacitors: Porous materials get energized. *Nat. Mater.* **16**, 161-162 (2017).

17. Miller J. R., Outlow R. A. & Holloway B. C. Graphene Double-Layer Capacitor with ac Line-Filtering Performance. *Science* **329**, 1637-1639 (2010).

18. Pech D., et al. Ultrahigh-power micrometre-sized supercapacitors based on onion-like carbon. *Nat. Nanotech.* **5**, 651-654 (2010).

19. Sheng K., et al. Ultrahigh-rate supercapacitors based on eletrochemically reduced graphene oxide for ac line-filtering. *Sci. Rep.* **2**, 247 (2012).

20. Lin J., et al. 3-Dimensional graphene carbon nanotube carpet-based microsupercapacitors with high electrochemical performance. *Nano Lett.* **13**, 72-78 (2013).

21. Wu Z. S., et al. Ultrathin Printable Graphene Supercapacitors with AC Line-Filtering Performance. *Adv. Mater.* **27**, 3669-3675 (2015).

22. Rangom Y., Tang X. T. & Nazar L. F. Carbon Nanotube-Based Supercapacitors with Excellent ac Line Filtering and Rate Capability via Improved Interfacial Impedance. *ACS Nano* **9**, 7248-7255 (2015).

23. Senthilkumar S. T., Wang Y. & Huang H. Advances and prospects of fiber supercapacitors. *J. Mater. Chem. A* **3**, 20863-20879 (2015).

24. Gao K., et al. All Fiber Based Electrochemical Capacitor towards Wearable AC Line Filters with Outstanding Rate Capability. *Chem. Electro. Chem.* **6**, 1450-1457 (2019).

25. Zhou Q., et al. Nitrogen-Doped Holey Graphene Film-Based Ultrafast Electrochemical Capacitors. *ACS Appl. Mater. Inter.* **8**, 20741-20747 (2016).

26. Xu Y., et al. Holey graphene frameworks for highly efficient capacitive energy storage. *Nat. Commun.* **5**, 4554 (2014).

27. Islam N., et al. High-frequency electrochemical capacitors based on plasma pyrolyzed bacterial cellulose aerogel for current ripple filtering and pulse energy storage. *Nano Energy* **40**, 107-114 (2017).

28. Miller J. R. & Outlaw R. A. Vertically-Oriented Graphene Electric Double Layer Capacitor Designs. *J. Electrochem. Soc.* **162**, 5077-5082 (2015).

29. Zhang M., et al. From wood to thin porous carbon membrane: Ancient materials for modern ultrafast electrochemical capacitors in alternating current line filtering. *Energy Storage Mater.* **35**, 327-333 (2021).

30. Park J., Lee J. & Kim W. Water-in-Salt Electrolyte Enables Ultrafast Supercapacitors for AC Line Filtering. *ACS Energy Lett.* **6**, 769-777 (2021).

31. Zhang H., et al. Hybridized Graphene for Supercapacitors: Beyond the Limitation of Pure Graphene. *Small* **17**, e2007311 (2021).

32. Zhang C., et al. Ultrahigh-Rate Supercapacitor Based on Carbon Nano-Onion/Graphene Hybrid Structure toward Compact Alternating Current Filter. *Adv. Energy. Mater.* **10**, 2002132 (2020).

33. Ren G., et al. Ultrahigh-rate supercapacitors with large capacitance based on edge oriented graphene coated carbonized cellulous paper as flexible freestanding electrodes. *J. Power Sources* **325**, 152-160 (2016).

34. Ren G., et al. Kilohertz ultrafast electrochemical supercapacitors based on perpendicularly-oriented graphene grown inside of nickel foam. *Carbon* **71**, 94-101 (2014).

35. Cai M. Z., et al. Fast Response, vertically oriented graphene nanosheet electric double layer capacitors synthesized from C2H2. *ACS Nano* **8**, 5873-5882 (2014).

36. Cai M., et al. A high density of vertically-oriented graphenes for use in electric double layer capacitors. *Carbon* **50**, 5481-5488 (2012).

37. Premathilake D., et al. Fast Response, Carbon-Black-Coated, Vertically-Oriented Graphene Electric Double Layer Capacitors. *J. Electrochem. Soc.* **165**, 924-931 (2018).

38. Xu S., et al. Electric-Field-Assisted Growth of Vertical Graphene Arrays and the Application in Thermal Interface Materials. *Adv. Funct. Mater.* **30**, 2003302 (2020).

39. Levie R. D. On porous electrodes in electrolyte solutions: I. Capacitance effects.

Electrochimica Acta **8**, 751-780 (1963).

40. Ma H., et al. Graphene oxide induced hydrothermal carbonization of egg proteins for high-performance supercapacitors. *J. Mater. Chem. A* **5**, 17040-17047 (2017).

41. Ma H., et al. Tailoring the oxygenated groups of graphene hydrogels for high-performance supercapacitors with large areal mass loadings. *J. Mater. Chem. A* **6**, 6587-6594 (2018).

Supplementary Files

This is a list of supplementary files associated with this preprint. Click to download.

- NatureCommunicationsSupportingInformationXusc.docx